



HAL
open science

The zinc-binding motif of human RECQ5 β suppresses the intrinsic strand annealing activity of its DExH helicase domain and is essential for the helicase activity of the enzyme

Hua Ren, Shuo-Xing Dou, Xing-Dong Zhang, Peng-Ye Wang, Radhakrishnan Kanagaraj, Pavel Janscak, Jin-Shan Hu, Xu Guang Xi

► To cite this version:

Hua Ren, Shuo-Xing Dou, Xing-Dong Zhang, Peng-Ye Wang, Radhakrishnan Kanagaraj, et al.. The zinc-binding motif of human RECQ5 β suppresses the intrinsic strand annealing activity of its DExH helicase domain and is essential for the helicase activity of the enzyme. *Biochemical Journal*, 2008, 412 (3), pp.425-433. 10.1042/BJ20071150 . hal-00478878

HAL Id: hal-00478878

<https://hal.science/hal-00478878>

Submitted on 30 Apr 2010

HAL is a multi-disciplinary open access archive for the deposit and dissemination of scientific research documents, whether they are published or not. The documents may come from teaching and research institutions in France or abroad, or from public or private research centers.

L'archive ouverte pluridisciplinaire **HAL**, est destinée au dépôt et à la diffusion de documents scientifiques de niveau recherche, publiés ou non, émanant des établissements d'enseignement et de recherche français ou étrangers, des laboratoires publics ou privés.

The zinc-binding motif of human RECQ5 β suppresses the intrinsic strand annealing activity of its DExH helicase domain and is essential for the helicase activity of the enzyme

Hua Ren^{1,5}, Shuo-Xing Dou², Xing-Dong Zhang², Peng-Ye Wang², Radhakrishnan Kanagaraj³, Pavel Janscak³, Jin-Shan Hu^{4,*} and Xu Guang Xi^{5,*}

¹College of Life Science, East China Normal University, Science Bld., 3663 North Zhongshan Rd., Shanghai 200062, P. R. China

²Laboratory of Soft Matter Physics, Beijing National Laboratory for Condensed Matter Physics, Institute of Physics, Chinese Academy of Sciences, Beijing 100080, China

³Institute of Molecular Cancer Research, University of Zurich, Winterthurerstrasse 190, CH-8057 Zurich, Switzerland.

⁴Department of Basic Medical Sciences, College of Osteopathic Medicine of the Pacific, Western University of Health Sciences, 309 E. Second Street, Pomona, CA 91766, USA

⁵CNRS, UMR 2027, Institut Curie – Section de Recherche, Centre Universitaire, Bâtiment 110, F-91405 Orsay, France.

To whom correspondence should be addressed (e-mail jshu@westernu.edu or xuguang.xi@curie.u-psud.fr)

SUMMARY

RecQ family helicases, functioning as caretakers of genomic integrity, contain a zinc-binding motif which is highly conserved among these helicases, but does not have a substantial structural similarity with any other known zinc-finger folds. Here, we show that a truncated variant of the human RECQ5 β helicase comprised of the conserved helicase domain only, a splice variant named RECQ5b possesses neither ATPase nor DNA unwinding activities, but surprisingly displays a strong strand-annealing activity. In contrast, a fragment of RECQ5 β including the intact zinc-binding motif, which is located immediately downstream of the helicase domain, does not exhibit any strand-annealing activity and is proficient in DNA unwinding. Quantitative measurements indicate that the regulatory role of the zinc-binding motif is achieved by enhancing the DNA binding affinity of the enzyme. The novel intra-molecular modulation of RECQ5 β catalytic activity mediated by the zinc-binding motif may represent a universal regulation mode for all RecQ family helicases.

Key words: RecQ helicase, DNA unwinding, DNA annealing, zinc-finger motif, intra-molecular regulation.

Running title: Modulation of RECQ5 function by Zinc Finger

INTRODUCTION

DNA helicases are molecular motors that transduce the chemical energy derived from NTP hydrolysis into mechanical force to unwind double-stranded DNA (dsDNA) [1,2]. Therefore, helicases display both DNA-stimulated ATPase and ATP-dependent helicase activities. Structural studies revealed that helicases from superfamily 1 and 2 (SF1 and SF2) contain a structural module that consists of two RecA-related domains [3,4]. Residues involved in ATP binding/hydrolysis and DNA binding are located in the cleft separating the two RecA-like domains. It is postulated that these domains serve as a DNA translocation motor [4].

The RecQ family DNA helicase are highly conserved from bacteria to man and play essential roles in the maintenance of genomic stability [5-8]. In humans, five RecQ family members, namely RECQ1 [9,10], BLM [11], WRN [12], RECQ4 [13] and RECQ5 [14], have been identified. Defects in BLM, WRN and RECQ4 lead to human hereditary disorders: Bloom syndrome (BS), Werner syndrome (WRN) and Rothmund-Thompson syndrome (RTS), respectively, that are characterized by genome instability and cancer predisposition [15]. In addition to the highly conserved DExH helicase domain containing seven helicase motifs, most RecQ family helicases contain a unique RQC domain (RecQ conserved) which is composed of a zinc-binding motif and a winged helix-turn-helix (WH) motif [16,17]. RecQ helicase activity is highly regulated not only through inter-molecular protein-protein interactions [18], but also through intra-molecular interactions between different domains [19]. In this study, we have chosen the human RECQ5 protein as a model to study the functional modulation of the DExH-helicase core by the zinc-binding domain. The striking feature of human RECQ5 is that it exists in three different isoforms, namely RECQ5 α , RECQ5 β and RECQ5 γ , which result from alternative splicing of the RECQ5 transcript [14,20]. The three proteins are identical within the N-terminal region of 410 residues which constitutes the helicase domain with the conserved set of seven helicase motifs (Supplementary Figure 1). RECQ5 α is the shortest variant including only the helicase domain (410 amino acids). RECQ5 β contains the helicase domain and a putative RQC domain, which is followed by a long C-terminal region that shows no homology to the other RecQ helicases. RECQ5 γ includes the helicase domain followed by a C-terminal extension of 25 amino acids that is not present in RECQ5 β . At present, only RECQ5 β has been characterized biochemically [21]. It possesses both DNA-unwinding and DNA strand-annealing activities [21]. In addition, RECQ5 β has been shown to promote strand exchange on forked DNA

structures [22]. However, the molecular mechanism that underlies the coordination of DNA unwinding and strand-annealing activities of RECQ5 β remains largely elusive.

The RECQ5 α and RECQ5 β proteins offer an attractive model system to characterize the enzymatic activities of a RecQ helicase domain in isolation and in association with other sub-domains on the same polypeptide. This unique property allows us to address some interesting and important questions that have not yet been resolved with any DNA helicase. These questions include : (i) Is the helicase domain sufficient to catalyze dsDNA separation; (ii) Does the helicase domain have an intrinsic strand-annealing activity as suggested by its structural similarity to the strand-exchange protein RecA; (iii) What is the role of the accessory domains, namely the zinc-binding domain, in the helicase activity of the enzyme. In the present study, we found that the helicase domain of RECQ5 does not possess DNA-unwinding capability, but exhibits an intrinsic strand-annealing activity. More importantly, the zinc-binding motif is found to act as a molecular switch that suppresses the strand-annealing activity of the helicase domain and triggers DNA-unwinding activity through modulating DNA binding.

MATERIALS AND METHODS

Proteins and DNA substrates

The human RECQ5 α and RECQ5 β proteins were produced as C-terminal fusions with a self-cleaving chitin-binding domain and purified as previously described [21]. The truncation mutants of RECQ5 β were amplified by PCR and cloned into pET15b as N-terminal fusions with a hexa-histidine tag. The resulting plasmids were transformed into the *E. coli* strain BL21-codonPlus (Stratagene). The cells were grown to the mid-exponential phase (A_{600} of 0.5-0.6) at 37 °C and the protein expression was induced by 0.25 mM of isopropyl-D-thiogalactoside at 15 °C for 18 h. The cells were lysed in buffer containing 50 mM Tris-HCl (pH 7.5), 500 mM NaCl, 0.1% Triton X-100, PMSF 0.1 μ M and 10% ethylene glycerol. The cell lysate was clarified by centrifugation and the supernatant was applied to a 20 ml Ni²⁺-column connected to an ÄKTA FPLC system. The bound proteins were eluted with a linear gradient of imidazole (0.02-0.4 M; 300 ml). Fractions containing the proteins of interest were identified by SDS-PAGE. Proteins were further purified using size-exclusion chromatography (Superdex 200, Amersham). Human replication protein A (RPA) protein was produced and purified according to previously published procedure [23].

PAGE purified DNA oligonucleotides (Supplementary Table 1) were purchased from Proligo. The DNA duplex substrates were prepared as described previously [24]. Briefly, 250 μ M component oligonucleotides were denatured in the 1 \times TE buffer containing 1 M NaCl or KCl by heating at 95 °C for 10 min. The denatured DNA was then annealed at 37 °C for 48 h. The annealed products were separated on 8% native PAGE containing 10 mM KCl run at 4 °C for 12 h with constant current of 20 mA.

Quantification of protein-bound Zn²⁺ ion

Protein-bound Zn²⁺ ion was measured using 4-(2-pyridylazo)resorcinol (PAR), a reporter dye that absorbs light at 490 nm when bound to Zn²⁺. To precisely quantify the Zn²⁺ content, all buffers were treated with Chelex[®]-100 resin (Bio-Rad). The proteins were dialysed against the EDTA-free Chelex[®]-treated buffer, passed over a 10-cm column of Chelex[®]-100 and re-concentrated. To facilitate the Zn²⁺ release, the protein (about 1 nmole in 40 μ l) was first denatured with Chelex[®]-treated 7 M guanidine-HCl, and then transferred to a 1-ml cuvette. PAR was added to the cuvette to a final concentration of 100 μ M and the volume was adjusted to 1 ml with PAR buffer containing 20 mM Tris-HCl (pH 8.0) and 150 mM NaCl. The absorbance was recorded from 300 to 600 nm on an UVIKON

spectrophotometer 941 (Kontron) at 25 °C. The quantity of Zn^{2+} was determined using the absorbance coefficient for the $Zn(PAR)_2$ complex ($\epsilon_{500} = 6.6 \times 10^4 \text{ M}^{-1} \text{ cm}^{-1}$). As a control, 20 nmoles of the pure $ZnCl_2$ was quantified under the identical conditions.

ATP binding assay

2'(3')-*O*-(*N*-methanthraniloyl) adenosine-5'-triphosphate, a fluorescent nucleotide analogue of ATP (mantATP), was used to determine the apparent dissociation constant for ATP binding by RECQ5 proteins. For that purpose, the fluorescence spectra of the proteins at a concentration of 0.5 μM were first measured using FluoroMax-2 spectrofluorimeter (Jobin Yvon, Spex Instruments S.A., Inc) at 25 °C in a 10×10×40 mm quartz cuvette. The proteins were excited at 280 nm and their intrinsic fluorescence emission near 350 nm was monitored. This measurement was useful for confirming the overlap of the fluorescence emission spectra of the proteins and the excitation spectrum of mantATP near 350 nm. When excited at 280 nm, this overlap would result in, due to FRET, an enhancement of the emission of mantATP at 440 nm after its binding to the proteins.

The mantATP binding assay was performed by using a Bio-Logic auto-titrator (TCU-250) and a Bio-Logic optical system (MOS450/AF-CD) in fluorescence mode. Varying amounts of mantATP were added to 1 ml of binding buffer containing 0.5 μM protein. After 1 minute incubation, fluorescence at 440 nm was measured. Titrations were performed in a temperature-controlled cuvette at 25 °C. The solution was stirred continuously by a magnetic stir bar during the whole titration process. The apparent dissociation constant K_d was determined by fitting the fluorescence intensity at 440 nm (corrected for the inner filter effect) with Equation 1,

$$F = F_s c_d + f_d x + f_c \frac{(x + 0.5c_d + K_d) - \sqrt{(x + 0.5c_d + K_d)^2 - 4 \times 0.5c_d \times x}}{2}, \quad (\text{Equation 1})$$

where, F_s is the starting fluorescence of the reaction mixture, f_d is the fluorescence coefficient of free mantATP, f_c is the fluorescence coefficient of the complex formed, x is the total concentration of mantATP. $c_d = V_0 / (V_0 + V_i) \cong 1 - x / [\text{mantATP}]$ is included to correct accurately for the sample dilution effect, where V_0 is the initial sample volume, V_i is the volume of titrant added, and $[\text{mantATP}]$ is the mantATP concentration of the titrant.

ATPase assay

The ATPase activity of the RECQ5 proteins was determined by measuring the concentration of inorganic phosphate produced by ATP hydrolysis [25]. The reaction was carried out in ATPase reaction buffer (50 mM Tris-HCl, pH 8.0, 3 mM MgCl₂, 0.5 mM DTT) at 37 °C in a volume of 100 µl. The reactions were initiated by the addition of enzyme into a reaction mixture containing 1.5 µM heat-denatured Hind III-cut pGEM-7Zf linear DNA and the mixture of ATP and [γ -³²P]ATP. The reaction was stopped by adding 0.2 ml of the stopping buffer containing 8.1 mM ammonium molybdate and 0.8 M HCl. The liberated ³²P_i was extracted with a solution of 2-butanol/benzene/acetone/ammonium molybdate (750:750:15:1) saturated with water. An aliquot of 60 µl was removed from the organic phase and the radioactivity was quantified using a liquid scintillation counter.

DNA binding assays

DNA binding of RECQ5 proteins was analyzed by fluorescence polarization anisotropy assay as described previously [24]. The DNA binding assay was performed using the Bio-Logic auto-titrator (TCU-250) and the Bio-Logic optical system (MOS450/AF-CD) in a fluorescence anisotropy mode. Varying amounts of proteins were added to 1 ml of binding buffer containing 1 nM DNA substrate. After 1-minute incubation, the fluorescence polarization anisotropy was measured. The temperature was controlled at 25 °C and the solution was stirred continuously during the whole titration process. The equilibrium dissociation constant was determined by fitting the data to the Michaelis-Menten or Hill equation using the program KaleidaGraph (Synergy Software).

DNA helicase assays

DNA unwinding reactions were carried out at 37 °C in 20 µl of the mixture containing 25 mM HEPES-NaOH, pH 7.5, 25 mM NaOAc, 7.5 mM Mg(OAc)₂, 2 mM ATP, 1 mM DTT, 0.1 mg/ml BSA, and indicated ³²P-labelled partial DNA duplex substrate (10 fmol, 3000 c.p.m./fmol). Where required, RPA was added at the indicated concentration. The reaction was initiated by addition of the indicated concentration of the RECQ5 protein and incubated at 37 °C for 30 minutes. Reactions were terminated by the addition of 5 µl of 5× loading buffer (50 mM EDTA, 0.5% SDS, 0.1% xylene cyanol, 0.1% bromophenol blue and 50% glycerol). The reaction products were resolved on a 12% (w/v) PAGE run in a TBE buffer (90 mM Tris, 90

mM boric acid, pH 8.3, and 1 mM EDTA) at 100 V for 2 h at 4 °C. Radiolabelled species were visualized using a Storm 860 Phosphoimager (Amersham Biosciences).

Stopped-flow DNA unwinding assay was performed according to Zhang et al. [26]. Briefly, the experiment was carried out using a Bio-logic SFM-400 mixer with a 1.5 mm×1.5 mm cell (Bio-Logic, FC-15) and a Bio-Logic MOS450/AF-CD optical system equipped with a 150-W mercury-xenon lamp. Fluorescein was excited at 492 nm, and its emission was monitored at 525 nm. The unwinding assay was performed in a two-syringe-mixing mode, where the protein and dsDNA substrates were preincubated in syringe #1 for 5 min, while ATP was present in syringe #4. Both syringes contained the unwinding reaction buffer (25 mM Tris-HCl, pH 7.5, 50 mM NaCl, 1 mM MgCl₂ and 0.1 mM DTT). The unwinding reaction was initiated by a rapid mixing of the contents of the two syringes. The dsDNA substrates had both strands labeled with fluorescein and hexachlorofluorescein, respectively, and their sequences are listed in the Supplementary Table 1. During the unwinding process, the fluorescein emission signal at 525 nm was enhanced due to the loss of FRET, i.e., the separation of the two dye molecules on the two ssDNA. For converting the output signal change from volts to percentage of unwinding, a calibration experiment was performed in a four-syringe-mixing mode, where the helicase in syringe #1, hexachlorofluorescein-labeled ssDNA in syringe #2, fluorescein-labeled ssDNA in syringe #3, and ATP in syringe #4, all incubated in unwinding reaction buffer. The fluorescent signal of the mixed solution from the four syringes corresponded to 100% unwinding. The standard reaction was carried out at 25 °C.

DNA strand-annealing assay

The DNA annealing activity of the RECQ5 isoforms was assayed using complementary synthetic oligonucleotides (0.5 nM) with one strand 5'-end labelled using [γ -³²P]ATP and T4 polynucleotide kinase. In this assay, the labelled oligonucleotide was added to reaction buffer (20 μ l) containing 20 mM Tris-acetate, pH 7.9, 50 mM KOAc, 10 mM Mg(OAc)₂, 1 mM DTT, 50 μ g/ml BSA and the indicated protein concentration. Where required, ATP, ATP γ S, AMPPNP or ADP were also added to a final concentration of 2 mM. The reaction was initiated by adding the unlabelled oligonucleotide and incubated at 37 °C for 30 minutes. The resulting DNA products were analysed as described for the helicase reactions.

The stopped-flow DNA strand-annealing assay was carried out under similar conditions as the helicase assay. The reaction was performed in a three-syringe-mixing mode,

where the helicase was in syringe #1 while fluorescein- and hexachlorofluorescein-labeled complementary ssDNA in syringe #2 and syringe #3, respectively, in buffer containing 25 mM Tris-HCl, pH 7.5, 50 mM NaCl, 1 mM MgCl₂ and 0.1 mM DTT. The sequences of the two 45-mer ssDNA substrates are indicated in the Supplementary Table 1. The reaction was initiated by rapidly mixing the contents of the three syringes. During the annealing process, the fluorescein emission signal at 525 nm was reduced due to FRET from fluorescein to hexachlorofluorescein on the two ssDNA. For converting the output signal change from volts to percentage of annealing, we performed another experiment in a two-syringe-mixing mode, where the helicase was in syringe #1 and the annealed dsDNA in syringe #4, both in the same buffer as indicated above. The fluorescent signal of the mixed solution from the two syringes corresponded to 100% annealing. The reaction was carried out 25 °C.

RESULTS AND DISCUSSION

RECQ5 helicase domain alone catalyzes strand annealing, but not strand separation

To analyze the function of an isolated helicase domain of RecQ DNA helicases, we investigated the biochemical properties the human RECQ5 α protein. We first compared the unwinding activities of RECQ5 α and RECQ5 β using gel-shift-based helicase assay. The results showed that RECQ5 β efficiently unwound a partial DNA duplex in a dose-dependent manner, whereas RECQ5 α displayed hardly detectable helicase activity, even in the presence of human RPA which was reported to stimulate RECQ5 β -mediated DNA unwinding [21] (Figure 1A and data not shown). To confirm this result, we employed a FRET-based helicase assay, which allowed the helicase-mediated DNA unwinding to be monitored in real time in a stop-flow experiment [26]. Consistent with earlier studies, RECQ5 α displayed non-detectable helicase activity, whereas RECQ5 β unwound the DNA substrate efficiently (Figure 1B). Under multiple-turnover conditions, the unwinding kinetics of RECQ5 β was biphasic. The fitting using a sum of two exponential terms gave two rate constants of 4.54 and 0.84 min⁻¹ for the fast and slow phases, respectively (Figure 1B and Table 1).

Next, we tested RECQ5 α and RECQ5 β for the ability to promote strand-annealing using two complementary 50-mer oligonucleotides. Remarkably, RECQ5 α was found to promote strand annealing as efficiently as RECQ5 β (Figure 2A). This result was rather surprising since the strand-annealing activity of RECQ5 β was shown to reside in the C-terminal portion of the RECQ5 β polypeptide [21]. We then examined the effect of ATP on the annealing activities of the RECQ5 proteins. Consistent with the previously published results, we found that ATP had no effect on the annealing activity of RECQ5 β , whereas ATP γ S, a poorly hydrolysable analogue of ATP, dramatically suppressed this reaction (Figure 2B, lanes 2 and 3). In contrast, ATP dramatically inhibited the annealing activity of RECQ5 α as it did ATP γ S (Figure 2B, lanes 8 and 9). We also examined the effect of ADP on the strand-annealing activities RECQ5 α and RECQ5 β . We found that ADP partially inhibited the annealing activity of RECQ5 β , but had no effect on the annealing activity of RECQ5 α (Figure 2B, lanes 4 and 10). Since previous studies showed that RPA efficiently inhibited the strand-annealing activities of RECQ5 β and RECQ1 [21,27], we also tested the effect of this single-strand binding protein on the strand-annealing activity of RECQ5 α . We found that similar to RECQ5 β , RECQ5 α -mediated strand annealing activity was inhibited by RPA in a dose-dependant manner (Figure 2C).

To quantitatively compare the DNA annealing kinetics of the RECQ5 isoforms, a FRET-based assay was used, which was essentially identical to the stop-flow helicase assay described above. The only difference was that the annealing assay monitored the decrease, instead of the increase, in the fluorescence emission due to FRET (Figure 2D). The measured annealing reaction rates were 0.95 min^{-1} and 0.14 min^{-1} for RECQ5 β and RECQ5 α , respectively. Thus, RECQ5 β promoted strand annealing about seven-fold faster than RECQ5 α (Figure 2E). However, when evaluated by the extent of annealing, RECQ5 α was more active than RECQ5 β (Figure 2E and Table 1).

In order to understand the molecular basis of the RECQ5 α -mediated strand annealing, we studied the quaternary structure of RECQ5 α in the absence and in the presence of ATP and/or ssDNA by means of size-exclusion chromatography on a SuperdexTM 75 column. These experiments (see supporting information (SI) Table 2) revealed an apparent molecular mass of 50~58 kDa at all condition tested, indicating that RECQ5 α promotes strand annealing as a monomer (the predicted molecular mass of monomeric RECQ5 α is 46.3 kDa).

RECQ5 helicase domain binds ATP efficiently, but displays a poor ATPase activity

To understand why RECQ5 α does not catalyse DNA unwinding, we analyzed its ATP-binding and ATPase activities relative to RECQ5 β . To quantify ATP-binding of RECQ5 α and RECQ5 β , mantATP, a fluorescent analogue of ATP, was used. The apparent dissociation constants (K_d) measured were 48.4 ± 2.5 and $51.0 \pm 4.9 \text{ }\mu\text{M}$ for RECQ5 α and RECQ5 β , respectively (Figure 3A and Table 1), indicating that the two isoforms bind ATP with a similar affinity.

The ATPase activities of the RECQ5 proteins were determined by measuring the release of inorganic $^{32}\text{P}_i$ from ATP in the presence of denatured dsDNA (2.9 kb) (Figure 3B). In agreement with previously published data [21], RECQ5 β was found to exhibit a robust ATPase activity, with a k_{cat} of $15.6 \pm 1.4 \text{ sec}^{-1}$. However, under identical conditions, RECQ5 α had no measurable ATPase activity (Figure 3B and Table 1).

These data indicate that the inability of RECQ5 α to unwind DNA is caused by its failure to hydrolyze ATP. Moreover, these data provide explanation for the differential effect of ATP on the strand-annealing activities of RECQ5 α and RECQ5 β (Figure 2B). As RECQ5 α can not hydrolyze ATP, it would persist in ATP-bound form, which is not proficient in strand annealing [21]. In the case of RECQ5 β , this inhibitory effect can be seen only with poorly hydrolysable ATP γS .

Zinc-binding motif is essential for the helicase activity of RECQ5 β

The observation that the isolated helicase domain of RECQ5 β failed to unwind dsDNA suggested a role for a C-terminal part of RECQ5 β in performing its helicase function. Therefore, C-terminal truncation mutants of RECQ5 β , including RECQ5 β ¹⁻⁴⁷⁵ and RECQ5 β ¹⁻⁶⁶², were assayed to identify the C-terminal region responsible for the intramolecular stimulation of the helicase activity of RECQ5 β . We found that these two mutants had essentially identical ATPase and DNA unwinding activities with respect to the full-length RECQ5 β protein (Figure 3B, Figure 5 and Table 1). Together, these observations suggest that the region of RECQ5 β spanning the amino acid residues 410-475 that constitute the putative zinc-binding domain (Figure 4A) plays an essential role in the ATPase and helicase activities of the enzyme. Molecular modelling of the zinc-binding motif of RECQ5 β revealed that the distances between the cysteine side-chain sulphur groups and the zinc atom for Cys⁴¹¹ (2.46 Å), Cys⁴²⁷ (2.36 Å), Cys⁴³¹ (2.42 Å), and Cys⁴³⁴ (2.39 Å) are close to the ideal distance (2.35 \pm 0.09 Å) for structural metal zinc-coordination sites [28] (Figure 4B). In agreement with this prediction, using PAR assay, we found that RECQ5 β contains 0.98 \pm 0.18 equivalent Zn²⁺ ion (Figure 4C and Table 1). The similar results were obtained for RECQ5 β ¹⁻⁴⁷⁵ and RECQ5 β ¹⁻⁶⁶² deletion mutants (Table 1). In contrast, the PAR assay indicated that RECQ5 α did not contain any Zn²⁺ ion, with measured Zn²⁺ value of 0.03 \pm 0.02 (Table 1).

To further evaluate the role of the zinc-binding motif in the helicase function of RECQ5 β , we generated a panel of mutants in which one or more of the four conserved cysteine residues were replaced by serine. However, these mutant proteins either formed aggregates or were degraded except for the C431S mutant, which was subjected to biochemical analysis. We found that the replacement of Cys⁴³¹ with Ser reduced the protein-bound Zn²⁺ to 0.35 \pm 0.12 equivalents (Table 1). Accordingly, this mutant had a significantly reduced ATPase and helicase activities relative to wild-type RECQ5 β (Figure 1B, Figure 3B and Table 1). Taken together, these data suggest that the zinc-binding motif modulates the enzymatic activity of RECQ5 β : it suppresses the strand-annealing function of the helicase domain and promotes strand separation.

Molecular mechanism of intra-molecular stimulation of the helicase activity of RECQ5 by the zinc-binding motif

In order to understand the molecular mechanism underlying the essential role of the zinc-binding motif in the helicase activity of RECQ5 β , we compared the DNA binding properties of RECQ5 α and RECQ5 β using fluorescence polarization assay with fluorescently-labelled oligonucleotide substrates [24]. This method allows direct measuring of DNA binding in solution under equilibrium conditions. K_d values for RECQ5 α and RECQ5 β determined from protein titration curves, indicated that RECQ5 α displayed much lower binding affinities for ss- and dsDNA than RECQ5 β (Figure 5 and Table 1).

It has been shown that ATP binding stimulates DNA binding of some helicases, which in turn triggers ATP hydrolysis [29-32]. Therefore, we measured the DNA binding activities of RECQ5 proteins in the presence of a non-hydrolyzable ATP analogue, AMPPNP and/or ATP γ S. We found that the ssDNA binding affinity of RECQ5 β was enhanced about 2–3 fold in the presence of 2 mM AMPPNP, whereas no noticeable effect could be observed with RECQ5 α , even in the presence of ATP (ATP cannot be hydrolyzed by RECQ5 α) (results not shown). These data imply that in RECQ5 α , there is no co-operativity between the ATP and DNA-binding sites.

To further explore the role of the zinc-binding motif in DNA binding by RECQ5 β , the RECQ5 β ¹⁻⁴⁷⁵ and RECQ5 β ¹⁻⁶⁶² truncation mutants were assayed for their DNA-binding activities. We found that these two mutants had similar DNA-binding affinities as the wild-type RECQ5 β protein, suggesting that the non-conserved C-terminal region of RECQ5 β does not play a role in DNA binding by the enzyme and that the zinc-binding motif confers the DNA-binding proficiency to the RECQ5 β helicase core (Figures 5A, 5B and Table 1).

To determine whether the zinc-binding motif of RECQ5 β is directly involved in DNA binding, we sought to examine the DNA binding properties of the isolated zinc-binding domain. Our first attempts to generate a fragment including only the zinc-binding fold (RECQ5 β ³⁷⁹⁻⁴⁵⁴) failed because this protein was found to be rapidly degraded. We then performed DNA binding experiments with RECQ5 β ³⁷⁹⁻⁶⁶² and RECQ5 β ⁴⁵⁴⁻⁶⁶² that could be purified to homogeneity. We found that RECQ5 β ³⁷⁹⁻⁶⁶², which contains the intact zinc-binding motif, was bound to DNA showing a preference for dsDNA (K_d values of 149 \pm 6.7 nM and 680 \pm 63 nM for dsDNA and ssDNA, respectively). In contrast, RECQ5 β ⁴⁵⁴⁻⁶⁶² with a truncated zinc-binding motif displayed hardly detectable DNA binding activity (Figures 5C and 5D). Together, these experiments revealed that the zinc-binding domain enhances the DNA-binding affinity of the RECQ5 β helicase core through direct DNA binding.

Model for the role of zinc-binding motif in the function of RecQ helicases

Based on the results presented above in combination with structural information for SF2 helicases, we proposed a model for the function of the zinc-binding motif of RecQ DNA helicases in DNA unwinding (Figure 6). Crystal structures of several DNA helicases including the *E. coli* RecQ helicase core suggested that ATP is bound at the top of domain 1A, while the ssDNA substrate is bound at the bottom of domains 1A and 2A (Figure 6). Since more residues in domain 1A are implicated in DNA binding than in domain 2A, as revealed by the crystal structures of NS3 helicase [33] and DEAD-Box helicase Vasa [34], it is likely that DNA may be bound more tightly to domain 1A than to domain 2A. Consequently, the portion of DNA that is bound to domain 2A may undergo large conformational fluctuation. In this case, the distance between the two helicase domains is too far to interact with each other to form the functional ATPase site that is essential for DNA unwinding. However, it is conceivable that while domain 1A binds ssDNA tightly, domain 2A can capture another ssDNA molecule. Thus, RECQ5 α would function as a ‘molecular crowding agent’ [35] that increases the effective concentrations of ssDNA substrates, thereby promoting the hybridization between complementary ssDNA molecules (Figure 6). However, in the presence of the zinc-binding motif, the double-stranded part of the DNA substrate would be tightly bound to the enzyme, enhancing the ssDNA binding to domain 2A (Figure 6). The tight binding of DNA to domain 1A and 2A, in collaboration with ATP binding, brings the domains into the closed form. In this structure, ATP is efficiently hydrolyzed and the energy is coupled to DNA unwinding.

Concluding remarks

The zinc-binding motif conserved among the RecQ family helicases does not have substantial structural similarity with any other known zinc-finger folds. It is therefore important to determine its specific function in the RecQ helicase family. We have previously shown that the zinc-binding motifs of *E. coli* RecQ and human BLM are important for DNA binding and protein folding of these helicases [25,36]. Thus, there is a clear correlation between the presence of the zinc-binding motif and the helicase activity of RecQ helicases. Interestingly, the human RECQ4 protein, the only RecQ family member without zinc-binding motif, fails to unwind DNA, but catalyzes DNA annealing, which is in agreement with our data obtained with RECQ5 α [37]. Thus, all of these studies establish the RecQ-specific zinc-binding motif as an essential DNA-binding module required for the RecQ family helicase activity.

FOOTNOTES

We thank Dr. Pascal Rigolet for help with molecular modeling, Drs. Robert Pansu and Loussiné Zargarian for assistance in the fluorescence measurements. We are grateful to Jilin Liu, Yan He and Nicolas Bazeille for carrying some preliminary studies. This research was supported by the grants from Institut National du Cancer and La Ligue Contre Le Cancer to X. G. X.; the National Natural Science Foundation of China and the Innovation Project of the Chinese Academy of Sciences; the Swiss National Science Foundation to P.J.; and the grants from the American Cancer Society (RSG-03-238-01) and the American Heart Association (RSG-03-238-01) to J.-S. H.

The abbreviations used are: dsDNA, double-stranded DNA; ssDNA, single-stranded DNA; EMSA, electrophoretic mobility shift assay; FRET, fluorescence resonance energy transfer; HRDC, helicase-and-ribonuclease D-C-terminal domain; mantATP, 2'(3')-*O*-(*N*-methlanthraniloyl) adenosine-5'-triphosphate; PAR, 4-(2-pyridylazo)resorcinol; RPA, replication protein A; RQC, RecQ carboxy-terminal conserved; WH, winged helix-turn-helix.

COMPETING INTERESTS STATEMENT

The authors declare that they have no competing financial interests.

REFERENCES

- 1 Lohman, T.M. and Bjornson, K.P. (1996) Mechanisms of helicase-catalyzed DNA unwinding. *Annu. Rev. Biochem.* **65**, 169-214
- 2 Soultanas, P. and Wigley, D.B. (2000) DNA helicases: 'inching forward'. *Curr. Opin. Struct. Biol.* **10**, 124-128
- 3 Caruthers, J.M. and McKay, D.B. (2002) Helicase structure and mechanism. *Curr. Opin. Struct. Biol.* **12**, 123-133
- 4 Singleton, M.R. and Wigley, D.B. (2002) Modularity and specialization in superfamily 1 and 2 helicases. *J. Bacteriol.* **184**, 1819-1826
- 5 Yamagata, K., Kato, J., Shimamoto, A., Goto, M., Furuichi, Y., and Ikeda, H. (1998) Bloom's and Werner's syndrome genes suppress hyperrecombination in yeast *sgs1* mutant: implication for genomic instability in human diseases. *Proc. Natl. Acad. Sci. U. S. A* **95**, 8733-8738
- 6 Hanada, K., Ukita, T., Kohno, Y., Saito, K., Kato, J., and Ikeda, H. (1997) RecQ DNA helicase is a suppressor of illegitimate recombination in *Escherichia coli*. *Proc. Natl. Acad. Sci. U. S. A* **94**, 3860-3865
- 7 Hickson, I.D. (2003) RecQ helicases: caretakers of the genome. *Nat. Rev. Cancer* **3**, 169-178
- 8 Mankouri, H.W. and Hickson, I.D. (2004) Understanding the roles of RecQ helicases in the maintenance of genome integrity and suppression of tumorigenesis. *Biochem. Soc. Trans.* **32**, 957-958
- 9 Puranam, K.L. and Blackshear, P.J. (1994) Cloning and characterization of RECQL, a potential human homologue of the *Escherichia coli* DNA helicase RecQ. *J. Biol. Chem.* **269**, 29838-29845
- 10 Seki, M., Miyazawa, H., Tada, S., Yanagisawa, J., Yamaoka, T., Hoshino, S., Ozawa, K., Eki, T., Nogami, M., Okumura, K. et al. (1994) Molecular cloning of cDNA encoding human DNA helicase Q1 which has homology to *Escherichia coli* Rec Q helicase and localization of the gene at chromosome 12p12. *Nucleic Acids Res.* **22**, 4566-4573
- 11 Ellis, N.A., Groden, J., Ye, T.Z., Straughen, J., Lennon, D.J., Ciocci, S., Proytcheva, M., and German, J. (1995) The Bloom's syndrome gene product is homologous to RecQ helicases. *Cell* **83**, 655-666.
- 12 Yu, C.E., Oshima, J., Fu, Y.H., Wijsman, E.M., Hisama, F., Alisch, R., Matthews, S., Nakura, J., Miki, T., Ouais, S. et al. (1996) Positional cloning of the Werner's syndrome gene. *Science* **272**, 258-262

- 13 Kitao, S., Ohsugi, I., Ichikawa, K., Goto, M., Furuichi, Y., and Shimamoto, A. (1998) Cloning of two new human helicase genes of the RecQ family: biological significance of multiple species in higher eukaryotes. *Genomics* **54**, 443-452
- 14 Shimamoto, A., Nishikawa, K., Kitao, S., and Furuichi, Y. (2000) Human RecQ5beta, a large isomer of RecQ5 DNA helicase, localizes in the nucleoplasm and interacts with topoisomerases 3alpha and 3beta. *Nucleic Acids Res.* **28**, 1647-1655
- 15 Karow, J.K., Wu, L., and Hickson, I.D. (2000) RecQ family helicases: roles in cancer and aging. *Curr. Opin. Genet. Dev.* **10**, 32-38
- 16 Morozov, V., Mushegian, A.R., Koonin, E.V., and Bork, P. (1997) A putative nucleic acid-binding domain in Bloom's and Werner's syndrome helicases. *Trends Biochem. Sci.* **22**, 417-418
- 17 Bernstein, D.A., Zittel, M.C., and Keck, J.L. (2003) High-resolution structure of the E. coli RecQ helicase catalytic core. *EMBO J.* **22**, 4910-4921
- 18 Bachrati, C.Z. and Hickson, I.D. (2003) RecQ helicases: suppressors of tumorigenesis and premature aging. *Biochem. J.* **374**, 577-606
- 19 Hu, J.S., Feng, H., Zeng, W., Lin, G.X., and Xi, X.G. (2005) Solution structure of a multifunctional DNA- and protein-binding motif of human Werner syndrome protein. *Proc. Natl. Acad. Sci. U. S. A* **102**, 18379-18384
- 20 Sekelsky, J.J., Brodsky, M.H., Rubin, G.M., and Hawley, R.S. (1999) Drosophila and human RecQ5 exist in different isoforms generated by alternative splicing. *Nucleic Acids Res.* **27**, 3762-3769
- 21 Garcia, P.L., Liu, Y., Jiricny, J., West, S.C., and Janscak, P. (2004) Human RECQ5beta, a protein with DNA helicase and strand-annealing activities in a single polypeptide. *EMBO J.* **23**, 2882-2891
- 22 Kanagaraj, R., Saydam, N., Garcia, P.L., Zheng, L., and Janscak, P. (2006) Human RECQ5beta helicase promotes strand exchange on synthetic DNA structures resembling a stalled replication fork. *Nucleic Acids Res.* **34**, 5217-5231
- 23 Henricksen, L.A., Umbrecht, C.B., and Wold, M.S. (1994) Recombinant replication protein A: expression, complex formation, and functional characterization. *J. Biol. Chem.* **269**, 11121-11132
- 24 Dou, S.X., Wang, P.Y., Xu, H.Q., and Xi, X.G. (2004) The DNA binding properties of the Escherichia coli RecQ helicase. *J. Biol. Chem.* **279**, 6354-6363
- 25 Guo, R.B., Rigolet, P., Zargarian, L., Femandjian, S., and Xi, X.G. (2005). Structural and functional characterizations reveal the importance of a zinc binding domain in Bloom's syndrome helicase. *Nucleic Acids Res.* **33**, 3109-3124
- 26 Zhang, X.D., Dou, S.X., Xie, P., Wang, P.Y., and Xi, X.G. (2005) RecQ helicase-catalyzed DNA unwinding detected by fluorescence resonance energy transfer. *Acta Biochim. Biophys. Sin. (Shanghai)* **37**, 593-600

- 27 Sharma, S., Sommers, J.A., Choudhary, S., Faulkner, J.K., Cui, S., Andreoli, L., Muzzolini, L., Vindigni, A., and Brosh, R.M., Jr. (2005) Biochemical analysis of the DNA unwinding and strand annealing activities catalyzed by human RECQ1. *J. Biol. Chem.* **280**, 28072-28084
- 28 Alberts, I.L., Nadassy, K., and Wodak, S.J. (1998) Analysis of zinc binding sites in protein crystal structures. *Protein Sci.* **7**, 1700-1716
- 29 Wong, I. and Lohman, T.M. (1992) Allosteric effects of nucleotide cofactors on *Escherichia coli* Rep helicase-DNA binding. *Science* **256**, 350-355
- 30 Jezewska, M.J. and Bujalowski, W. (1996) Global conformational transitions in *Escherichia coli* primary replicative helicase DnaB protein induced by ATP, ADP, and single-stranded DNA binding. Multiple conformational states of the helicase hexamer. *J. Biol. Chem.* **271**, 4261-4265
- 31 Jezewska, M.J. and Bujalowski, W. (2000) Interactions of *Escherichia coli* replicative helicase PriA protein with single-stranded DNA. *Biochemistry* **39**, 10454-10467
- 32 Bujalowski, W. and Jezewska, M.J. (2000) Kinetic mechanism of nucleotide cofactor binding to *Escherichia coli* replicative helicase DnaB protein. stopped-flow kinetic studies using fluorescent, ribose-, and base-modified nucleotide analogues. *Biochemistry* **39**, 2106-2122
- 33 Kim, J.L., Morgenstern, K.A., Griffith, J.P., Dwyer, M.D., Thomson, J.A., Murcko, M.A., Lin, C., and Caron, P.R. (1998) Hepatitis C virus NS3 RNA helicase domain with a bound oligonucleotide: the crystal structure provides insights into the mode of unwinding. *Structure*. **6**, 89-100
- 34 Sengoku, T., Nureki, O., Nakamura, A., Kobayashi, S., and Yokoyama, S. (2006). Structural Basis for RNA Unwinding by the DEAD-Box Protein *Drosophila* Vasa. *Cell* **125**, 287-300
- 35 Minton, A.P. (1997) Influence of excluded volume upon macromolecular structure and associations in 'crowded' media. *Curr. Opin. Biotechnol.* **8**, 65-69
- 36 Liu, J.L., Rigolet, P., Dou, S.X., Wang, P.Y., and Xi, X.G. (2004) The zinc finger motif of *Escherichia coli* RecQ is implicated in both DNA binding and protein folding. *J. Biol. Chem.* **279**, 42794-42802
- 37 Macris, M.A., Krejci, L., Bussen, W., Shimamoto, A., and Sung, P. (2005) Biochemical characterization of the RECQ4 protein, mutated in Rothmund-Thomson syndrome. *DNA Repair (Amst)*. **5**, 172-180

Table 1 Summary of the measured parameters for RECQ5 isoforms and mutants

Protein	[Zn ²⁺]/[P]	ATP binding K _d (μM)	Annealing (%)	ATPase k _{cat} (s ⁻¹)	Helicase activity		DNA binding	
					(%)	k _{obs} (min ⁻¹)	K _d for ssDNA (nM)	K _d for dsDNA (nM)
RECQ5α	0.03 ± 0.02	48.4 ± 2.5	95.2 ± 8.6	ND	ND	ND	1.0 × 10 ⁶ ± 219 ^b	1.8 × 10 ⁶ ± 267 ^b
RECQ5β	0.98 ± 0.18	51.0 ± 4.9	72.3 ± 5.6	15.6 ± 1.4	84.1 ± 3.5	4.54 and 0.84 ^a	46.6 ± 2.7	59.3 ± 2.0
RECQ5β ^{C431S}	0.35 ± 0.12		78.6 ± 3.5	4.8 ± 0.6	58.3 ± 2.8	0.50 and 0.03 ^a	67.5 ± 10.1	201 ± 23.4
RECQ5β ¹⁻⁴⁷⁵	0.96 ± 0.11		25.5 ± 6.5	14.8 ± 1.1	90.3 ± 4.9	5.03 and 0.87 ^a	64.2 ± 5.1	79.8 ± 2.4
RECQ5β ¹⁻⁶⁶²	1.02 ± 0.15		55.3 ± 10.5	16.3 ± 1.3	92.5 ± 5.6	5.65 and 0.92 ^a	55.8 ± 2.1	70.3 ± 3.2
RECQ5β ³⁷⁹⁻⁶⁶²	1.01 ± 0.14						680 ± 60	149 ± 6.7
RECQ5β ⁴⁵⁴⁻⁶⁶²							1308 ± 6	1539 ± 32

^a Values corresponding to the fast rate constant and the slow rate constant, respectively.

^b DNA binding affinity is determined with K_d^{appa}=218.17±7.8 nM and Hn= 2.68±0.18 for dsDNA and K_d^{appa}=140±8 nM and Hn=2.76 for ssDNA using equation, K_d=(K_d^{appa})^(Hn).

THIS IS NOT THE FINAL VERSION. See doi:10.1093/bj/BJ20071150

Stage 2(a) POST-PRINT

FIGURE LEGENDS

Figure 1 Helicase assays of RECQ5 α and RECQ5 β

(A) Gel-based assay of DNA unwinding using 0.5 nM [5'-³²P]-labelled 23-base DNA duplex (UA/UB). Reactions were carried out at 37 °C for 30 minutes under condition as described in Materials and Methods. The reaction products were analyzed by 12% non-denaturing PAGE. (B) Stopped-flow DNA unwinding assay. As described in Materials and Methods, 1 nM 56:16-mer DNA substrate (UFA/UFB) was pre-incubated with 20 nM helicase for 5 min at 25 °C. Unwinding reaction was initiated by mixing with 1 mM ATP. The fluorescence emission of fluorescein at 520 nm (excited at 492 nm) was monitored. The increase of the fluorescence signal of fluorescein at 525 nm (excited at 492 nm) during unwinding was monitored. Fraction of DNA unwound was obtained by normalization of the fluorescence signal F using the value F_{\max} as obtained from the calibration measurement that corresponded to 100% unwinding (see Materials and Methods), i.e., Fraction unwound = $(F - F_s) / (F_{\max} - F_s)$, where F_s is the fluorescence signal at the start of unwinding.

Figure 2 RECQ5-mediated ssDNA annealing

(A) Annealing of the [5'-³²P]-labelled SPA (0.5 nM) and SPB ssDNA substrates by RECQ5 α and RECQ5 β . Reactions were incubated with the indicated protein concentrations for 30 min at 37 °C. The reaction products were separated by 12% non-denaturing PAGE and visualized by PhosphoImager. (B) Effect of nucleotides on the RECQ5-mediated ssDNA annealing. The reactions contained 50 nM RECQ5 α or RECQ5 β and were carried under the same conditions as in (A). Preformed 50 bp duplex and 50mer ss-oligonucleotide were loaded as markers (C1 and C2 respectively). The nucleotides as indicated were present in a concentration of 2 mM. (C) Strand-annealing activity of RECQ5 α and RECQ5 β in the presence of the increasing concentration of RPA. The complementary 50-mer oligonucleotides (0.5 nM) were incubated with or without RPA for 5 min at room temperature. The RECQ5 proteins were added to a final concentration of 40 nM and incubation was continued at 37 °C for 20 min. Reaction products were analyzed as in (A) and quantified using Image Quant software. The results are the average of three independent experiments. (D) FRET-based ssDNA-annealing assay. The annealing was measured by monitoring the decrease in fluorescence at 520 nm caused by FRET between fluorescein and

hexachlorofluorescein labels on the oligonucleotide substrates as indicated. Reaction contained 0.5 nM fluorescein-labeled SPFA DNA, 0.5 nM hexachlorofluorescein-labeled complementary SPFB DNA and 30 nM RECQ5 β . (E) Time course of ssDNA annealing by RECQ5 α and RECQ5 β proteins measured by the assay in (C). Proteins were present at a concentration of 30 nM. Fraction of annealed DNA (Table 1) was obtained by normalization of fluorescence signal F using the value F_{\min} as obtained from the calibration measurement that corresponded to 100% annealing (see Materials and Methods), i.e., Fraction annealed = $(F_s - F)/(F_s - F_{\min})$, where F_s is the fluorescence signal at the start of annealing.

Figure 3 ATP-binding affinity and ATPase activity of RECQ5 proteins

(A) Changes in fluorescence intensity at 440 nm as 0.5 μ M RECQ5 α and RECQ5 β , respectively, were titrated with increasing concentration of mantATP. Solid lines represent the best fit of the data to Equation 1. Apparent K_d values are summarized in Table 1. (B) ATPase activities of wild-type and mutant RECQ5 proteins. The initial rate of ATP hydrolysis by RECQ5 proteins is plotted as function of the ATP concentration. Reactions contained 250 nM RECQ5 protein and 1.5 μ M heated dsDNA and were carried out as described in Materials and Methods. The lines in the graph correspond to the best fits by Michaelis-Menten equation: $V = V_{\max} [ATP]/(K_M + [ATP])$, where V is the initial reaction rate, $[ATP]$ is the concentration of ATP, and K_M is the Michaelis-Menten constant. Each value represents the mean of at least three independent measurements.

Figure 4 Identification of the zinc-binding motif of RECQ5 β helicase

(A) Amino acid sequence alignment of the zinc-binding domains of RecQ family helicases. The multiple sequence alignment was performed using ClustalW software and refined manually. The conserved Cys and other residues are highlighted in red and blue, respectively. (B) Ribbon diagram showing the zinc-binding domain of the RECQ5 β helicase as revealed by molecular modelling based on the crystal structure of *E. coli* RecQ. The zinc ion is in cyan. The positions of the four conserved cysteine residues are labelled as C1 to C4. The conserved arginine, aspartic acid and aromatic residues, involved in three very important hydrogen-bonds (dashed lines) that stabilize the conformation of the zinc-binding domain are shown in ball and stick

representation. (C) Plot of concentration of protein-bound Zn^{2+} against RECQ5 β protein concentration as determined by PAR assay. The absorption spectra were scanned from 300 to 600 nm at 25 °C. As a control, 20 nmol $ZnCl_2$ complexed with PAR was scanned under the identical conditions.

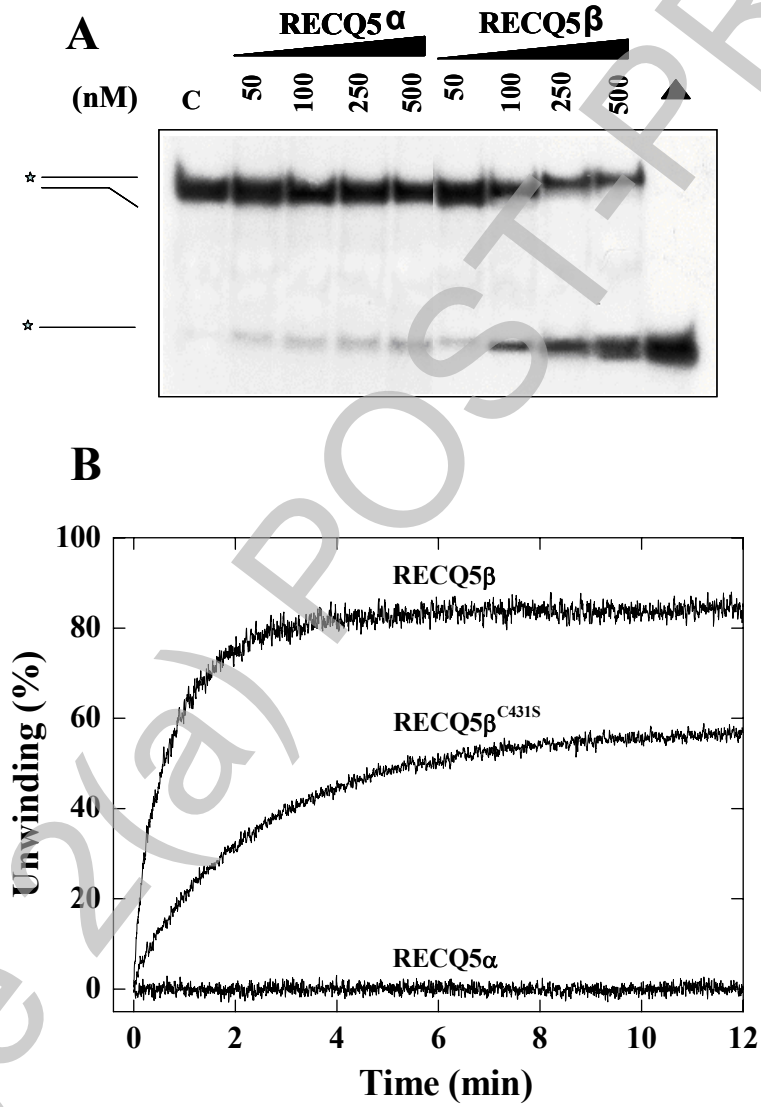
Figure 5 DNA binding activities of wild-type and mutant RECQ5 proteins

The anisotropy-based binding isotherms were obtained by varying protein concentration in the presence of 5 nM 3'-fluorescently labelled (A and C) ssDNA (BA) and (B and D) dsDNA (BA/BB). The data were fitted by Michaelis-Menten or Hill equations. The apparent K_d values are summarized in Table 1.

Figure 6 Model for the role of zinc-binding motif in the function of a RecQ helicase

In the absence of the zinc-binding motif (left), the helicase domains bind ssDNA with low affinity. Although one part of ssDNA binds relatively tightly to the domain 1A, the other part of ssDNA may dissociate from domain 2A due to thermal fluctuation, providing an opportunity for domain 2A to capture a complementary ssDNA. In this situation, RECQ5 α brings the two complementary strands into close proximity, promoting the hybridization of the complementary ssDNA. In this state, although ATP is bound tightly to domain 1A, the distance between the domains 1A and 2A is too long to form a functional ATPase site. In the presence of the zinc-binding motif (ZBM; right), the DNA substrate is tightly bound to the enzyme through an additional interaction between the zinc-binding motif and the duplex region of the substrate, which stabilizes ssDNA binding to the domains 1A and 2A. This tight DNA binding induces conformational changes in the protein that bring the two helicase sub-domains into a closed form, allowing ATP hydrolysis, a prerequisite for the helicase function.

Fig. 1



THIS IS NOT THE FINAL VERSION - see doi:10.1042/BJ20071150

Fig. 2

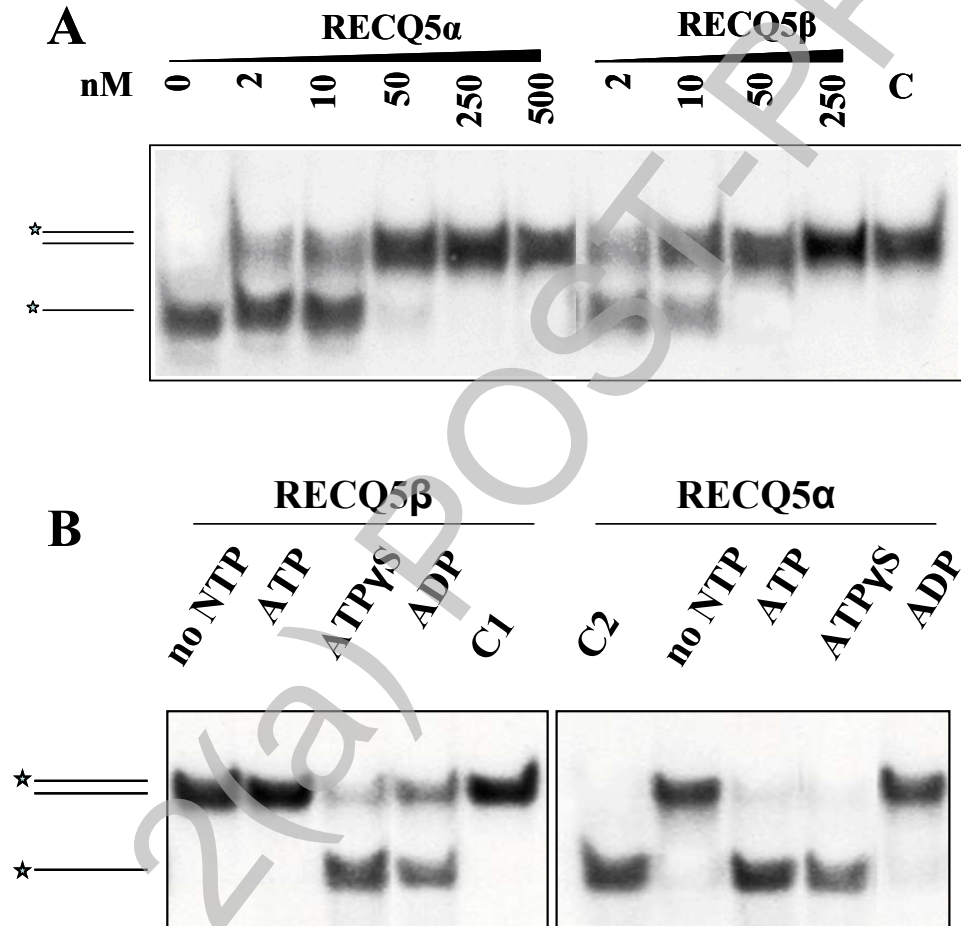


Fig. 2

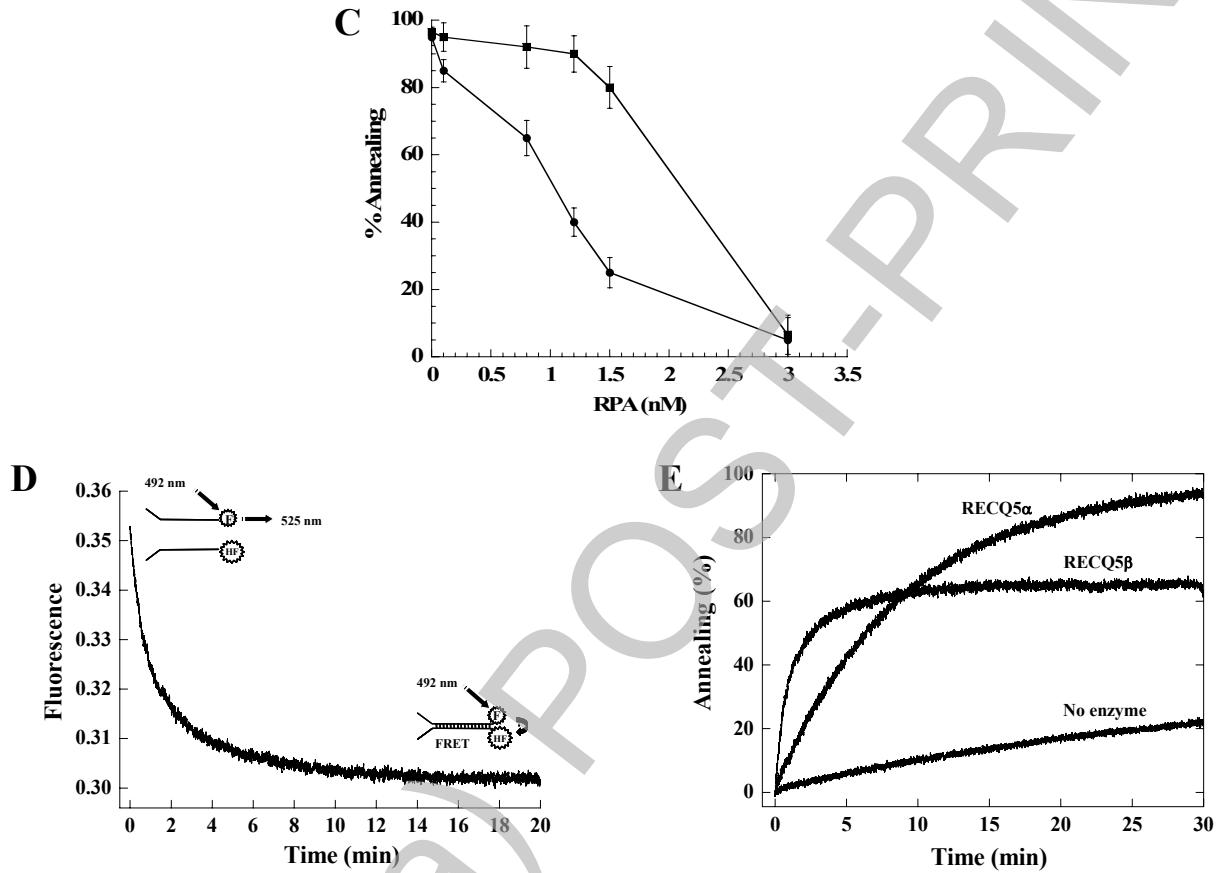


Fig. 3

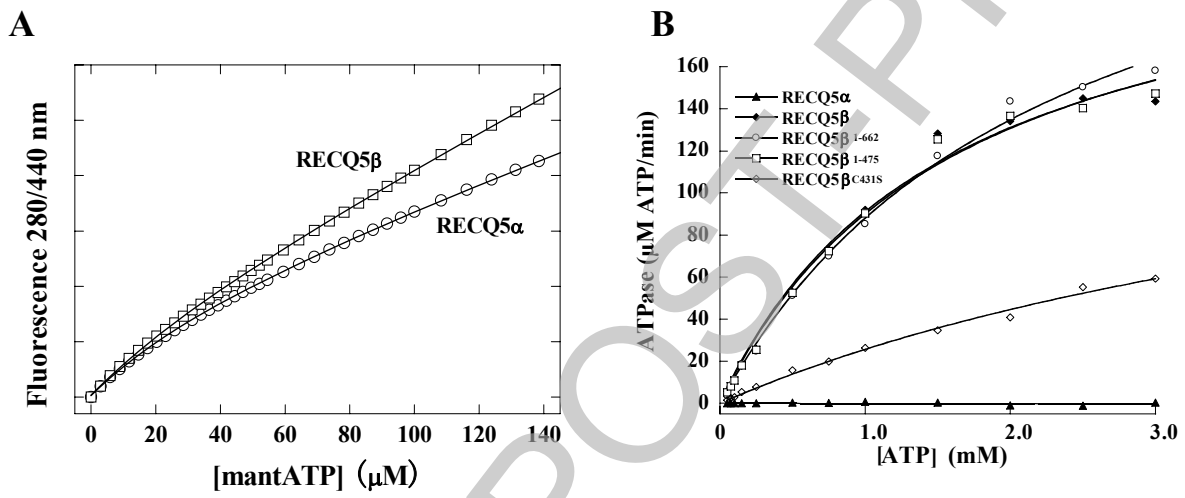


Fig. 4

A

hRECQ5	390	ASDKATIMAFDALVTFCEE-LGCRHAAIAKYFGDA---LPA CA KG----- CD H C Q N PTAVRRRLEALE
DmRECQ5	387	LLTERAIKQFEKITEFCER-TTCRHKLFSDFFGDP---TPD C SGQ----- CD V C KRPKKA E KALEMFH
BLM	1013	HTRETHFNLYSMVHYCENIT TC RR I QLLAY F GENGFNPDF CK KHP-DVS- CD N C CKTKDYKT--RDVT
RECQ1	433	---NVGQQKLYEMVSYCQNISK CR RV L MAQH F DEV-WNSEA C NKM----- CD N C CKDSAFER--KNIT
RqhI	866	ETKERQRQMLRQVIQFCENKTD CR RKQV L AY F GEN-FDKV H CRKG----- CD I C CEEATYIK--QDMT
WRN	886	KFRLYK L KMMAKMEK L Y L HS-S R CR R Q I IL S H F EDK-QVQKAS L G I M G TEK C DN C R S RLD H CY S MDDSE
SgsI	1024	ENKEKHLNKLQQVMAYCDNVTD CR R K L V LSY F NED-FDSK L CHKN----- CD N C RNSANVIN--EE--
RecQ	357	QLQDIERHKLNAMGAF A E A -QT CR RLV L LN Y F G EG--RQ E PC G N----- CD I C LD P PKQYDGSTDAQ

B

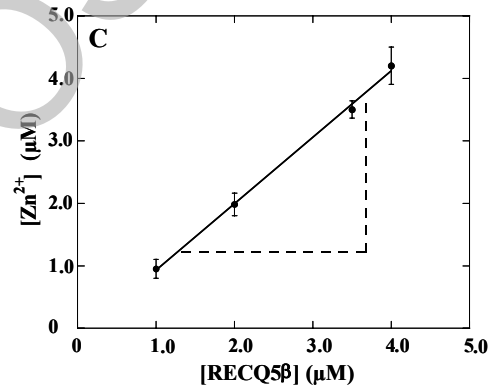
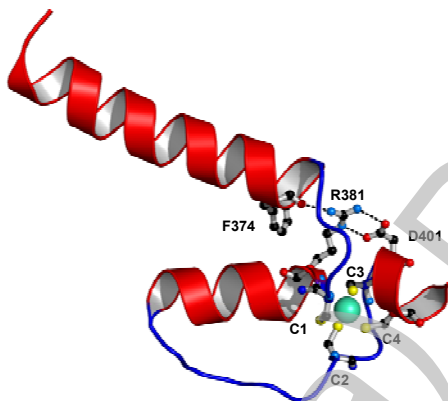


Fig. 5

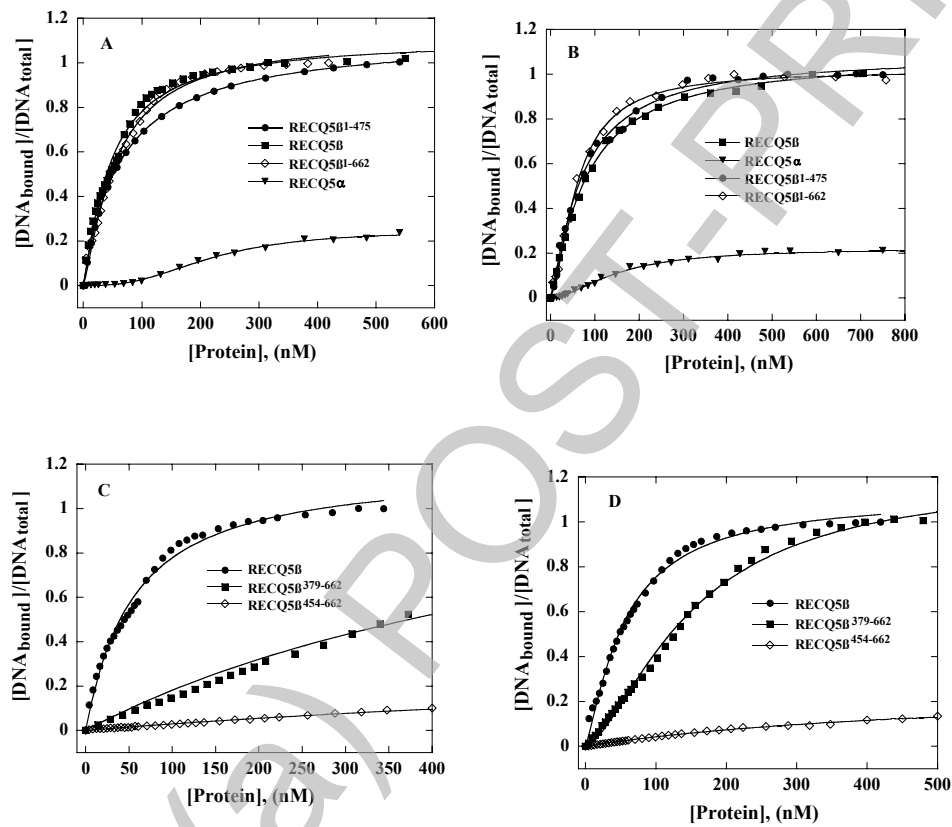


Fig. 6

